Structural studies on choline-carboxylate bio-ionic liquids by x-ray scattering and molecular dynamics

Luana Tanzi, Fabio Ramondo' , Ruggero Caminiti, Marco Campetella, Andrea Di Luca, and Lorenzo Gontrani'

Citation: J. Chem. Phys. **143**, 114506 (2015); doi: 10.1063/1.4931031
View online: http://dx.doi.org/10.1063/1.4931031
View Table of Contents: http://aip.scitation.org/toc/jcp/143/11
Published by the American Institute of Physics

Structural studies on choline-carboxylate bio-ionic liquids by x-ray scattering and molecular dynamics

Luana Tanzi,[1] Fabio Ramondo,[1,a)] Ruggero Caminiti,[2] Marco Campetella,[2]
Andrea Di Luca,[2] and Lorenzo Gontrani[2,b)]
[1]*Department of Physical and Chemical Sciences, University of L'Aquila, Via Vetoio, L'Aquila I-67100, Italy*
[2]*Department of Chemistry, University of Rome 'La Sapienza', P.le Aldo Moro 5, I-00185 Rome, Italy*

(Received 9 July 2015; accepted 24 August 2015; published online 16 September 2015)

We report a X-ray diffraction and molecular dynamics study on three choline-based bio-ionic liquids, choline formate, [Ch] [For], choline propanoate, [Ch][Pro], and choline butanoate, [Ch][But]. For the first time, this class of ionic liquids has been investigated by X-ray diffraction. Experimental and theoretical structure factors have been compared for each term of the series. Local structural organization has been obtained from *ab initio* calculations through static models of isolated ion pairs and dynamic simulations of small portions of liquids through twelve, ten, and nine ion pairs for [Ch][For], [Ch][Pro], and [Ch][But], respectively. All the theoretical models indicate that cations and anions are connected by strong hydrogen bonding and form stable ion pairs in the liquid that are reminiscent of the static *ab initio* ion pairs. Different structural aspects may affect the radial distribution function, like the local structure of ion pairs and the conformation of choline. When small portions of liquids have been simulated by dynamic quantum chemical methods, some key structural features of the X-ray radial distribution function were well reproduced whereas the classical force fields here applied did not entirely reproduce all the observed structural features. © *2015 AIP Publishing LLC.* [http://dx.doi.org/10.1063/1.4931031]

I. INTRODUCTION

Since their appearance 20 yr ago, ionic liquids (ILs) have constituted a class of technologically useful and fundamentally interesting materials for a variety of both scientific and applicative issues.[1–3] They are defined as salts with a melting point below the boiling temperature of water (100 °C). The wide range of possible cation-anion combinations enables ILs to be developed to have a specific set of physicochemical properties, conductivity, polarity, chemical and thermal stability, low flammability, oxidation resistance in air and excellent solvation power, or to be designed for particular applications. Among their properties, the negligibly low vapour pressure is the most prominent feature why they are considered as green solvent. However, concerns have risen on the potential toxicity and biodegradability of most of the currently studied ILs.[4] With the aim of reducing their impact on the environment, ILs entirely composed of biomaterials (BioILs) have been developed. They combine some of the excellent physicochemical properties of ILs with the advantage of biodegradable and not toxic starting materials. Additional advantages over ILs are their facile and green preparation, such as simple ion-exchange and/or acid/base reactions,[5] and the use of readily available and inexpensive starting materials. As early as 1960s, choline salicylate was observed to melt at about 50 °C.[6] More recently, several choline-based ionic liquids were prepared[7–9] suggesting that choline is an alternative to synthetic cations commonly used in ILs. Thus, starting from choline hydroxide, an essential water-soluble nutrient grouped within the B-complex vitamin, choline was coupled with suitable and halogen free anion species. The choice for anions was suggested by the relative low melting point of some salts composed by imidazolium, ammonium, or phosphonium cations and naturally derived anions such as those coming from carboxylic or amino acids.[10–15] A class of BioILs was therefore synthesized by combining choline cation with different amino acid anions;[12–14] as an alternative, the large variety of carboxylic acids of natural origin was the source to realize ionic compounds consisting of choline cation and carboxylic acid anions.[16] As it occurs for ILs, BioILs peculiar properties stem from the complexity of the nanoscopic interactions between their molecular constituents that include both long-range isotropic Coulombic forces and short-range van der Waals ones. In BioILs, the presence of anisotropic hydrogen bonds could strongly affect their properties. Strong hydrogen bonding may in fact occur between the carboxylate group of the anion and the hydroxyl group of the choline cation.

Despite the importance of BioILs, only few papers concerning these systems have been published so far. An analysis of the literature shows that most available studies deal with their synthesis,[5] their physical chemical properties,[17–19] and their reactions in low melting mixtures.[20] A few theoretical studies on choline benzoate and choline salicylate[21,22] and on choline coupled with a series of amino acid anions[23] have been reported. Recently, infrared and Raman spectra have been measured for three choline-carboxylic acid based BioILs and important structural features have been derived from molecular dynamics.[24] More recently, systems composed by alanine (the simplest amino acid)-choline[25] and proline-choline[26] pairs

a)Electronic mail: fabio.ramondo@univaq.it
b)Electronic mail: lorenzo.gontrani@uniroma1.it

have been investigated by X-Ray diffraction, IR spectroscopy, and molecular dynamics. Such studies[24–26] show that hydrogen bonding is a crucial feature in establishing the local geometric structure for these choline based liquids.

The main aim of the present work is to investigate the structure of some ionic liquids consisting of choline cation and carboxylic acid anions using for the first time X-Ray diffraction on BIoILs. In the present work, X-Ray diffraction patterns of three choline-based BioILs, choline formate, [Ch][For], choline propanoate, [Ch][Pro], and choline butanoate [Ch][But] (Figure 1) have been measured with our energy-dispersive X-ray diffractometer. This series of compounds allows us to compare structural features of BioILs containing carboxylate anions with short alkyl chains, such as propanoate and butanoate, and unsubstituted carboxylate anion, such as formate. As observed,[17] the physical properties of liquids are affected by the alkyl chain length for different reasons. For example, mesoscopic structures were observed for various ILs by X-Ray diffraction[27] and different interpretations of the corresponding spectra have been proposed.[28–32] Occurrence of structural heterogeneities was observed also for ILs containing short alkyl chains[33,34] and some diffraction pre-peaks were observed for small systems like choline-proline ionic liquid where strong ion-pairs were found and scattering of second-neighbor groups is expected.[26] On the other hand, the relaxing properties of alkyl groups are expected to affect the strength of the interaction between carboxylate and choline cation.

In the present study, we employ a combination of *ab initio* molecular dynamics (AIMD), classical MD, and experimental measurements with the aim of interpreting the geometric structure and the dynamics of the corresponding bulk liquid systems following an approach successfully applied to a wide number of ionic liquids.[25,26,35–37] Although the *ab initio* MD approach is much more computationally demanding than classical MD, it has the advantage to include, at least in principle, the exact interaction energy up to all the many body terms. In particular, a quantum-mechanical treatment is able to describe the complex polarization effects due to hydrogen bonding. Quantum chemistry using density functional approach has been therefore applied to the three systems first to characterize the zero kelvin structure of isolated ions and ion pairs. Density functional theory (DFT) has been then used to study dynamic effects and multiple aggregation and AIMD simulations were carried out on small portions of the liquid made up of several ion pairs. Theoretical diffraction patterns were calculated from AIMD simulations and compared with the X-Ray measured curves. In order to provide long range structural information, liquid structure was further studied by MD simulations on larger models employing classical force fields. Local structural organization has been compared with that obtained from *ab initio* calculations and theoretical radial distribution functions (RDFs) were last compared with experiment.

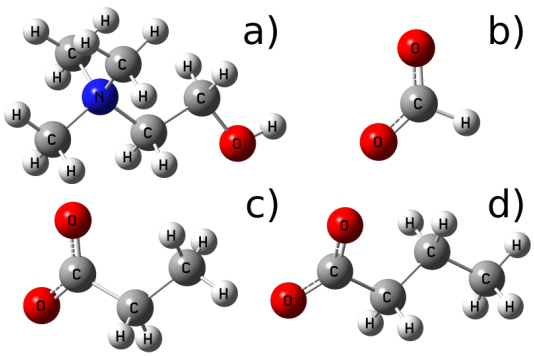

FIG. 1. Choline cation (a) and formate (b), propanoate (c) and butanoate (d) anions.

II. EXPERIMENTAL DETAILS

BioILs were synthesized by dropwise addition of the corresponding acid to a choline hydroxide solution as described in the previous study.[24]

The large angle X-ray scattering experiments were performed using the non-commercial energy-scanning diffractometer built in the Department of Chemistry at the University La Sapienza of Rome, Patent No. 01126484—23 June 1993. Detailed description of instrument, technique, and the experimental protocol (instrument geometry and scattering angles) of the data acquisition phase can be found in a series of papers by our group.[38–43] The appropriate measuring time (i.e., number of counts) was chosen to obtain scattering variable (q) spectra with high signal to noise ratio (500 000 counts on average).

The expression of q is

$$q = \frac{4\pi \sin(\theta)}{\lambda} = 1.014E \sin(\lambda), \tag{1}$$

where E is expressed in keV and q in Å^{-1}. The various angular data were processed according to the procedure described in the literature,[38–43] normalized to a stoichiometric unit of volume containing one ion pair and combined to yield the total "(static) structure factor," $I(q)$,

$$I(q) = I_{e.u.}(q) - \sum_{i=1}^{N} x_i f_i^2, \tag{2}$$

where f_i are the atomic scattering factors, x_i are the number concentrations of the i-type atoms in the stoichiometric unit (i.e., the group of particles used as reference for data normalization, the ion pair in this case), and $I_{e.u.}$ is the observed intensity in electron units (electrons^2).

Such function depends on the scattering contributions of all the particles of the system, according to the pairwise distances between them (in the case of X-rays, the atoms scatter the radiation through the electron clouds surrounding them). Therefore, this function gives a sort of mathematical picture of the spatial disposition of the sample atoms. Such spatial arrangement can be figured out by confronting the experimental structure factor with those derived from model systems.

This function is multiplied by q and q-dependent sharpening factor, $M(q)$ (with nitrogen as sharpening atom) to enhance the resolution of the curve at high q values and to decrease the truncation error in the calculation of the Fourier transform from the reciprocal space (q) to the direct one (r). The expression for $M(q)$ is

$$M(q) = \frac{f_N^2(0)}{f_N^2(q)} \exp(-0.01q^2). \tag{3}$$

Fourier transform of $qI(q)M(q)$ led to radial distribution function (r.d.f.)

$$D(r) = 4\pi r^2\rho_0 + \frac{2r}{\pi}\int_0^{q_{max}} qI(q)M(q)\sin(rq)dq, \quad (4)$$

where ρ_0 (electrons^2/Å^3) is the bulk number density. When the uniform distribution component is dropped ($4\pi r^2\rho_0$), we obtain the differential correlation function, $Diff(r)$, which contains only the structural contribution to the distribution function,

$$Diff(r) = D(r) - 4\pi r^2\rho_0. \quad (5)$$

III. COMPUTATIONAL DETAILS

A. Liquids by AIMD simulations

Quantum-mechanical calculation for ion pairs of [Ch][For], [Ch][Pro], and [Ch][But] was performed using the Gaussian 09 package.[44] Equilibrium geometries and vibrational frequencies were obtained using DFT methods with the B3LYP[45,46] exchange and correlation functional and employing the 6-311++G** basis set. A cationic cluster consisting of five ions, three choline cations and two propionate anions, was further considered and its geometry was determined at the B3LYP/6-311++G** level.

AIMD simulations were performed on models of 12 ion pairs for choline formate (12CHFOR), 10 ion pairs for choline propanoate (10CHPRO), and 9 ion pairs for choline butanoate (9CHBUT).

Simulations were performed using Born-Oppenheimer Molecular Dynamics (BOMD) method implemented in the CPMD code.[47] Potential energy calculations were carried out using Perdew, Burke and Ernzerhof (PBE) exchange-correlation functional[48] and a plane wave (PW) basis set. Plane waves expansion was developed in a periodic cubic box with unit cell edge of 13.87 Å for 12CHFOR, 14.00 Å for 10CHPRO, and 13.98 Å for 9CHBUT, with an energy cutoff of 70 Ry. Pseudopotential functions contain the dispersion-corrected atom-centered potentials[49] (DCACPs) in the norm-preserving Martins-Trouiller form.[50] Each simulation was started from a snapshot of classical MD simulation and each system was equilibrated for 5 ps in the NVT ensemble at 300 K using the Nosé-Hoover thermostat.[51–53] Trajectories were collected (saving coordinates every step) for 13 ps with a time step of 15 a.u. (0.3627 fs) in the NVE ensemble. Trajectories were then converted in xyz format.

B. Liquids by classical MD

A first series of simulations was carried out describing potential energy with the two-body Generalized Amber Force Field (GAFF)[54] using Gromacs v.4.6.2 package[55] as molecular dynamics engine. The initial configurations were generated randomly with the software Packmol[56] using a minimum interatomic separation of 2 Å as a constraint. Simulations were carried out starting from partial atomic charges obtained using the Restrained Electrostatic Potential (RESP) method[57,58] by fitting the electrostatic potential for isolated cations and anions at the equilibrium geometry calculated at the HF/6-31G* level. The use of HF/6-31G* method has been demonstrated to lead to the implicit polarization required in the additive FF model of condensed phase systems and complies with the rest of the GAFF parameter set, optimized to be compatible with the Cornell *et al.* families of Amber force fields[59] that implement this charge derivation scheme. We are aware that the charges calculated with HF are larger than those calculated with DFT, an issue that could be detrimental in the simulation of highly charged systems like ionic liquids. Yet, we chose to use HF electrostatic potential to ensure the maximum compatibility with GAFF parameters.

Electrostatic interactions were calculated using Particle Mesh Ewald (PME) under periodic boundary conditions and Linear Constraint Solver (LINCS) algorithm was applied to all bonds involving hydrogen atoms. Cutoff radii for van der Waals and direct-space Ewald interactions were set to 10 Å. Parallelization was carried out with domain decomposition strategy and Message Passing Interface (MPI) paradigm.

Effects of some simulation parameters were tested on [Ch][Pro]. The length of the box edge was evaluated on two systems composed, respectively, of 500 and 1200 ion pairs (CHPRO) and with cubic box edges of about 50 Å and 70 Å. Energy minimizations were performed using both steepest descent and conjugated gradient methods. Equilibration consisted in gradually heating the systems at 550 K in the NPT ensemble and then in cooling them to 300 K using Nosé-Hoover thermostat[51–53] and Parrinello-Rahman barostat[60–62] set to 1 atm. Equilibration time was about 1 ns and a relaxation period of 500 ps without using barostat. Subsequently, the systems were simulated in NVT ensemble for 3.5 ns with integration time step of 2 fs and trajectories were collected every 1000 steps. A similar simulation protocol was employed to test the effect of temperature with simulation runs at 500 K.

[Ch][For] and [Ch][But] were setup and simulated like CHPRO; systems were composed of 1500 ion pairs for choline formate (CHFOR) and 333 ion pairs for choline butanoate (CHBUT) and the length of cubic box edge was approximately 70 Å and 45 Å, respectively.

A second series of simulations was carried out by adding a three-body function to GAFF force field as proposed by the DREIDING force field[63] and hereafter indicated as GAFF_HB. DREIDING hydrogen bond function includes an explicit dependence of the energy on hydrogen bond angle and donor-acceptor distance. The parameters of the three body function are given in the supplementary material to this paper.[64] Gromacs is unable to manage such force field function and these sets of simulations were therefore run with DL_POLY 4 package.[65] System setup, i.e., initial coordinates and force field, was made using Aten v. 1.7 package;[66] the systems studied consist of 512 ion pairs of choline formate (CHFOR_HB), choline propanoate (CHPRO_HB), or choline butanoate (CHBUT_HB), placed in large cubic cells. Equilibration followed the same scheme described for GAFF simulations.

C. MD-derived structure factor

Molecular dynamics allows us to calculate theoretical structure factor from pair correlation functions $g_{ij}(r)$. In fact,

structure factor can be expressed with the following equation:[67]

$$I(q) = \sum_{i=1}^{N}\sum_{j=1}^{N} x_i x_j f_i(q) f_j(q) H_{ij}(q) \qquad (6)$$

in which $H_{ij}(q)$ are the partial structure factors, defined in terms of the pair correlation functions by the Fourier integral

$$H_{ij}(q) = 4\pi\rho_0 \int_0^{r_{max}} r^2[g_{ij}(r) - 1]\frac{\sin(qr)}{qr}dr, \qquad (7)$$

where r_{max} is half the box edge. The partial structure factors and the theoretical total structure factor were calculated with an in-house written code. Theoretical $I(q)$ was then multiplied by q and the sharpening factor, $M(q)$, to obtain a theoretical $qI(q)M(q)$ function comparable with the experimental one. Theoretical $D(r)$ and $Diff(r)$ were calculated as described in Sec. II for the experimental curves.

IV. RESULTS AND DISCUSSION

A. X-Ray results

The structure function of [Ch][Pro] is reproduced in Figure 2(a). It shows the broad peaks typically found in liquids, though the degree of ordering suggested by the intensity of the peaks is not at all negligible. Although the assignment of the peaks in reciprocal space is not directly feasible, since many interference patterns from the various scattering centers contribute to each peak, we can qualitatively state that the intramolecular scattering is responsible for almost all the observed intensity beyond 4 Å^{-1}, while intermolecular contacts originate the principal peak falling at about 1.6 Å^{-1} and the two smaller peaks around 2 and 3.8 Å^{-1}. These two features have been previously considered as a fingerprint of H-bond interactions.[68] Noteworthy, there are no peaks before the principal peak (the so-called "pre-peaks" or "FSDP"—First Sharp Diffraction Peak), whose presence, recognized in aqueous solutions of metal ions, in molecular as well as ionic liquids,[34] and in glasses and melts,[69] is generally attributed to the existence of a considerable degree of medium-range order of some kind in the liquid (MRO: ⩾10 – 20 Å). If the experimental radial distribution function is considered, Figure 2(b), after the two evident first two peaks falling at about 1.6 and 2.2 Å that are easily attributed to first-neighbor molecular peaks (i.e., atom directly bonded) and second-neighbors (1-3 contacts), respectively, three very broad peaks follow, at about 6, 11, and 16 Å, that are originated by all the intermolecular interactions of the solvation shells. In the range of 3-6 Å, some small peaklets corresponding to the furthest intramolecular contacts, 1-4 or beyond, or to highly correlated intermolecular interactions (e.g., strong hydrogen bonds) come out of the broad peak envelope. The spatial correlation of the system decays rapidly beyond 16.5 Å, in accordance with the absence of low-q peaks.

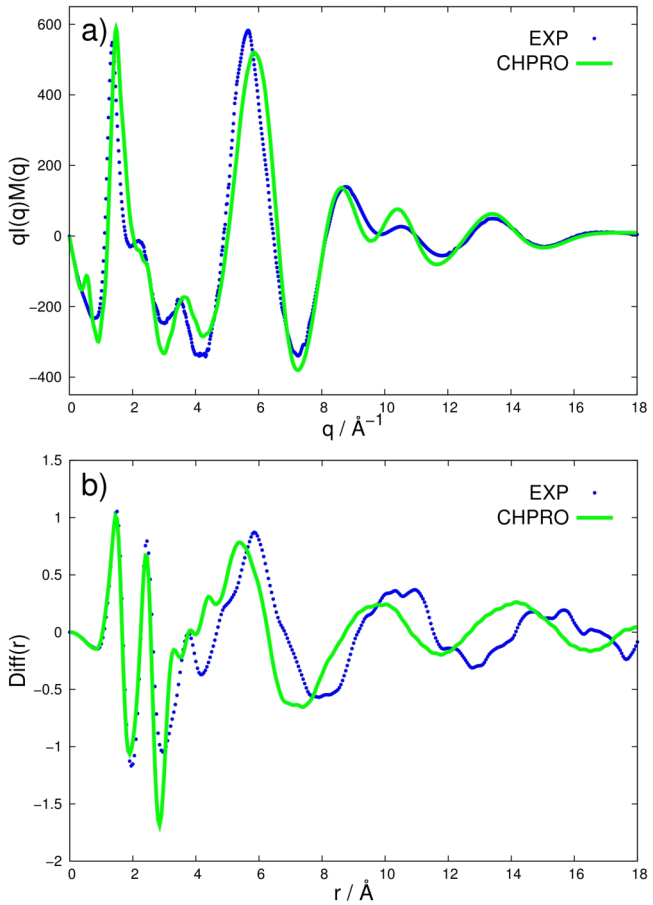

FIG. 2. Theoretical GAFF and experimental $qI(q)M(q)$ (a) and $Diff(r)$ (b) of [Ch][Pro].

B. X-Ray and *ab initio* results

Assignment of some peaks can be more easily obtained by analysing the cation-anion interactions through quantum chemical methods. The equilibrium structure of ion pairs in vacuo has been recently studied at MP2 and DFT levels of theory by some of us.[24] Actually, the electrostatic potential surface of choline reveals that cations could interact with anions through the OH group, a hydrogen bonding site, as well as the $N(CH_3)_3^+$ group, a Coulombic interaction site. Both the interactions have been now considered and two structures were localized on the potential energy surface, Figure 3; however, the strong OH···O hydrogen bonds between choline and carboxylate group should prevent the coordination at the $N(CH_3)_3^+$ groups. A structural feature common to all the coor-

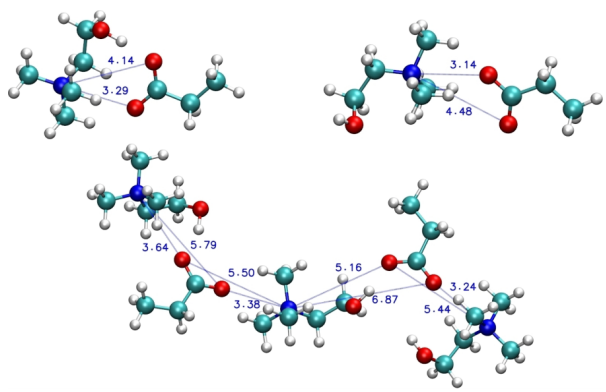

FIG. 3. *Ab initio* ion pairs and cluster of [Ch][Pro]: intermolecular distances at B3LYP/6-311++G** level.

dination structures is the presence of CH···O contacts. The cation-anion arrangement in isolated ion pairs allows therefore to maximize all intermolecular interactions starting from the electrostatic coulombic interactions, passing through the highly directional OH···O hydrogen bonding, and ending up to the weaker CH···O dipolar interactions. As previously reported,[24] the stability of hydrogen bonded ion pairs is comparable for all the three couples and consistently the coupling geometry is nearly the same. The cation-anion binding energy along with the hydrogen bond geometry is in addition very similar to those calculated for choline cation and amino acid anion pairs.[23,25,26] In addition, looking at the *ab initio* geometry of ion pairs (Figure 3), intermolecular N···O distances are expected at 3.2 and 4.2 Å in a zone where experimental $Diff(r)$ shows typical features, Figure 2(b).

On the other hand, we cannot exclude that ionic association involves simultaneously the OH and $N(CH_3)_3^+$ groups to form an alternation between cations and anions in the liquid. Figure 3 shows in fact that alternative structures of ion pairs, although with different stabilities, might coexist in liquid. We therefore proposed the pentamer in Figure 3 as a simple model where cations and anions are connected in alternation. Such an arrangement gives strong OH···O hydrogen bonds like in the ion pair and it additionally alternates cations and anions as usually observed in liquids.[70,71] As for the ion pair, some intermolecular N···O distances occur again in the range 3.8-4 Å in agreement with the observed peaks, Figure 2(b).

Starting from the *ab initio* results of the ion pairs, undoubtedly representative of local and direct interactions in liquids, we included dynamic aspects through AIMD simulations of small portions of liquid keeping a quantum mechanical level of treatment. Simulations of the small liquid systems, 12CHFOR, 10CHPRO, and 9CHBUT, confirm that ions are connected by stable hydrogen bonds. For a comparison with ion pair geometries, their structure was optimized again using the same plane wave basis set and the same functional, PBE/PW(70Ry), employed for AIMD simulations and hydrogen bond O···H appears shorter (1.55 Å) than B3LYP/6-311++G** values (1.66 Å and 1.65 Å).

The intermolecular RDFs between most representative atoms of choline cation and anion are given in Figure 4. Bearing in mind that our simulations are too short to give a full description of long time dynamics of hydrogen bonding, the narrow distribution of O···O values at around 2.6 Å is a clear evidence of the stability of hydrogen bonding. We can therefore identify ion pairs in our AIMD models with O···H distance of 1.60 Å for [Ch][For] and 1.58 Å for [Ch][Pro] and [Ch][But]. Noteworthy, our previsions are remarkably close to the distribution functions obtained for choline-aminoacids liquids.[23,25,26] In addition, we can state that the lengthening of the hydrogen bond distances in comparison with the values of 1.55 Å for isolated and static ion pairs (at level PBE/70Ry) is due to thermal motion. Similarly, secondary and weaker CH···O interactions are hindered by temperature effects, and consequently, the related CH···O contacts increase from 2.08–2.10 Å for isolated pairs to 2.22–2.21 Å in liquids. Figure 4 shows also a structure beyond the main peak that consists of two small peaks around 4-5 Å due to the bidentate nature of the carboxylate group as hydrogen bonding acceptor. Such structural feature is found in other ILs containing carboxylate.[23,25,26] Along with O···O intermolecular distances, Figure 4 presents the RDFs between nitrogen atoms of cations and oxygen atoms of anions. Such a RDF shows a broad peak around 4 Å. This correlation is due to the electrostatic interaction between the negative charge of oxygen atoms of anions and the positive charge localized on the nitrogen atom of choline cations. Such structured peak in the N···O intermolecular RDF is an important feature, common to carboxylate choline ILs,[25] that suggests how their structure shows an alternating pattern of anions and cations similar to the structure of the oligomer proposed in Figure 3.

In order to provide a better vision of the cationic and anionic distribution, we have calculated the Spatial Distribution Functions (SDFs) using the Trajectory Analyzer and Visualizer.[72] Figures 5(a)–5(c) report the SDFs of the choline hydroxyl hydrogen atoms around the carboxylate anion. The proton is well localized between the carboxylate acceptor and the oxygen of the choline cation. Due to the symmetry of the carboxylate group, there are different approaching directions for the cations. It is interesting to note that when one carboxylate atom is coordinated to form hydrogen bonding, the second oxygen may be also involved in another hydrogen bonds although at smaller extent. Figures 5(d)–5(f) report also SDFs of oxygen atoms of anions calculated with respect to the

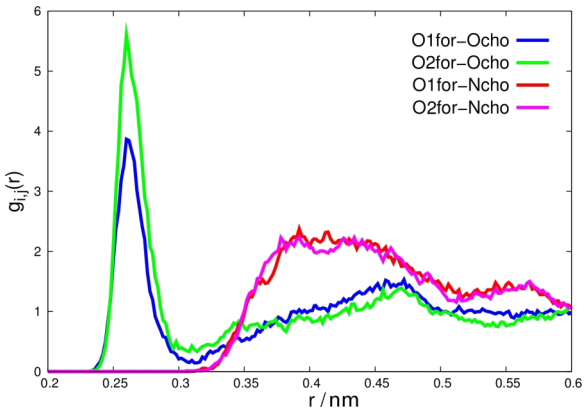

FIG. 4. Radial distribution functions between oxygen atoms of formate (O1 and O2) and choline (Ocho) and between formate oxygen (O1 and O2) and choline nitrogen (Ncho) atoms from AIMD simulations.

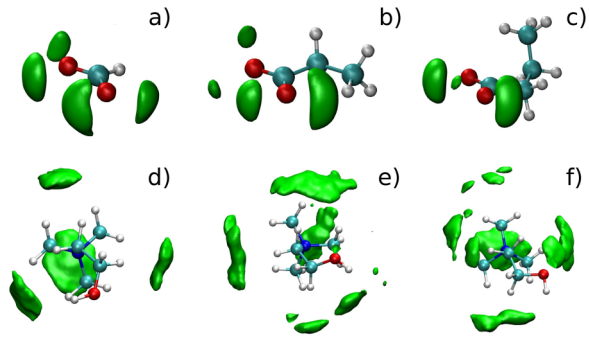

FIG. 5. Spatial distribution functions of choline hydroxyl hydrogen calculated with respect to the COO framework of formate (a), propanoate (b), and butanoate (c). Isosurface at level 70 is drawn. Spatial distribution functions of oxygen atoms of formate (d), propanoate (e), and butanoate (f) anions calculated with respect to the nitrogen atom of choline (cutoff 4.5). Isosurface at level 40 is drawn.

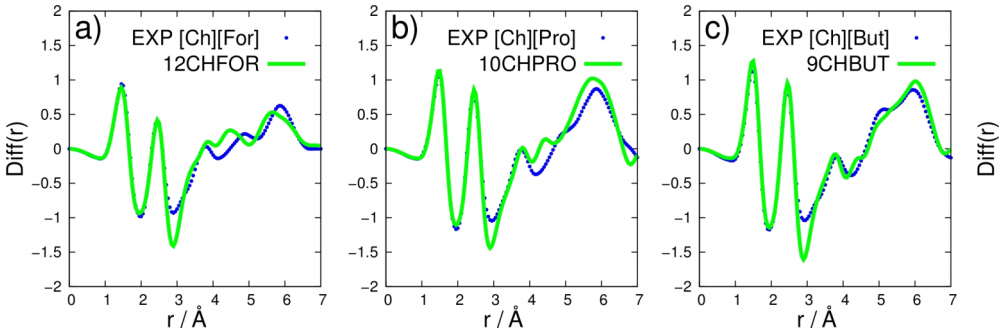

FIG. 6. *Diff*(r) at low r region from AIMD simulation of 12CHFOR (a), 10CHPRO (b), 9CHBUT (c), and comparison with experiment.

nitrogen of choline, an atom very close to the center of mass of the cation. Such SDFs reveal that the formate anion has some preferential approach directions whereas the propanoate and butanoate anions are more homogeneously distributed around the choline cation.

Since our AIMD models do not allow to investigate the liquid structure beyond the first interaction shell, we have calculated the *Diff*(r) curves up to 7 Å from AIMD simulations and compared them with the experimental data in Figure 6. It is very interesting to observe that for all the three compounds, *ab initio* MD simulations give good predictions of the experimental data in all ranges considered.

C. X-Ray results and MD simulations

Since AIMD models are too small to provide long range structural features and the application of *ab initio* molecular dynamics simulations on larger systems is still computationally prohibitive, we studied the liquid structure of the three compounds by MD simulations employing classical force fields, starting from the two-body GAFF one. The quality of the force field was tested against the liquid density as shown in Table I. Theoretical density of all the compounds is not in full agreement with experimental data. Nevertheless, we observe a decrease of density in agreement with the experimental trend found for propanoate, butanoate, and hexanoate series.[17] A second set of simulations was then performed imposing the experimental density to the systems. Structure factors were calculated from both the density series of simulations; however, the results seem to be quite insensitive to the liquid density.

$qI(q)M(q)$ derived from the last 5 ns molecular dynamics trajectory for [Ch][Pro] is compared in Figure 2(a) with the corresponding experimental curve; differential distribution functions *Diff*(r) are reported in Figure 2(b). From a quick inspection of Figure 2(a), we notice that the observed structure factor is not accurately reproduced by our models in all q regions. In particular, the peak at about 5.8 Å^{-1} is clearly shifted at higher values; in addition, our simulations show a very low peak (0.5 Å^{-1}) absent in the experiment. The presence of small spurious prepeaks in systems that do not show experimental ones could be a common thing in simulations of ionic liquids, especially if box is not very large and there are long distance truncation errors in radial distribution functions. On the other hand, the same GAFF force field does not predict prepeaks for formate as well as butanoate, in agreement with experimental evidences. A general better agreement emerges instead in the low-q range (1.8–2 Å^{-1}). Low accuracy is again found when *Diff*(r) functions are compared in Figure 2(b). We notice a good agreement on the range of intramolecular distances, whereas in the intermediate range, the experimental curves are shifted towards longer values. Another important observation regards the features of the large signal at 4.5 Å: simulations predict a large peak with four components whereas only two components and a shoulder are visible in the experimental curves.

TABLE I. Experimental and theoretical density, ρ (g/cm^3) of [Ch][For], [Ch][Pro], and [Ch][But]. Uncertainty is expressed as standard deviation in the last digit.

[Ch][For]	[Ch][Pro]	[Ch][But]	
1.16(1)[a]	1.0715(5)[17]	1.0465(5)[17]	Experimental
1.23(1)	1.14(1)	1.11(1)	GAFF 300 K
1.05(1)	1.02(1)	0.98(1)	GAFF_HB 300 K
1.01(1)	0.95(1)	0.94(1)	GAFF_HB 500 K

[a]This work.

To increase the mobility of the liquid and consequently reduce the structural order emerging from our theoretical model, we simulated the systems at higher temperature (500 K) (results are reported in the supplementary material[64]); however, the effect is indeed modest. The origin of these discrepancies should be found in the extent of cation-anion interactions, clearly overestimated in our models. The hydrogen bonding radial distribution curves obtained from GAFF simulations show that the average distance between acceptor and donor oxygens (2.54 Å) is markedly shorter than the *ab initio* values calculated from the ion pair (2.65 Å) in vacuo.[24] The two-body GAFF force field therefore largely overestimates the hydrogen bond interactions.

Several attempts were made to fit experimental data by scaling the partial charges of isolated ions by 0.8, as suggested by the charge transfer found in *ab initio* ion pairs, and by 0.5 or using partial charges found from the Mertz-Singh-Kollman calculations[73] for the ion pairs. Additional attempts were then made changing the σ and ϵ parameters of Lennard-Jones terms or introducing a σ value for hydrogen of hydroxyl group, absent in the original GAFF, however, no significant improvement was observed. Some results of such simulations can be found in the supplementary material to this paper.[64]

Since all the proposed changes did not improve significantly the agreement, we decided to maintain the generality of

TABLE II. Hydrogen bonding distances obtained from classical (GAFF and GAFF_HB) and AIMD simulations.

		[Ch][For]	
	AIMD	GAFF	GAFF_HB
$r_{O\cdots O}$ Å	2.61	2.54	2.68
$r_{OH\cdots O}$ Å	1.60	1.58	1.66
$r_{NCH\cdots O}$ Å	2.26	2.58	2.39
		[Ch][Pro]	
	AIMD	GAFF	GAFF_HB
$r_{O\cdots O}$ Å	2.66	2.54	2.66
$r_{OH\cdots O}$ Å	1.61	1.58	1.66
$r_{NCH\cdots O}$ Å	2.22	2.58	2.30
		[Ch][But]	
	AIMD	GAFF	GAFF_HB
$r_{O\cdots O}$ Å	2.62	2.50	2.66
$r_{OH\cdots O}$ Å	1.58	1.48	1.66
$r_{NCH\cdots O}$ Å	2.24	2.60	2.28

the GAFF force field and we added a three-body term centered on the acceptor-proton-donor triplets, as already followed for some protic ionic liquids.[68]

This additional term is supposed to weaken hydrogen bonding allowing the formation and dissociation of ion pairs more easily during simulation. A second important advantage of this term is the introduction of asymmetric features into hydrogen bonding. Simulations were carried out at the temperature of 400 K to enhance the agreement with the experimental data as found in the previous simulations.

As first observation, we note that the overestimation of long-range structure emerged from the two-body potential now disappears and hydrogen bond average distances calculated with the three-body potential are more similar to the *ab initio* values[24] (see Table II).

The structure factors (Figures 7(a)–7(c)) change upon introduction of the three-body term in the following points: (i) the peak at 4-6 $Å^{-1}$ appears now better reproduced and the maximum is now correctly predicted at about 5.8 $Å^{-1}$; (ii) the peak at lower q values, although well centered in q, does not

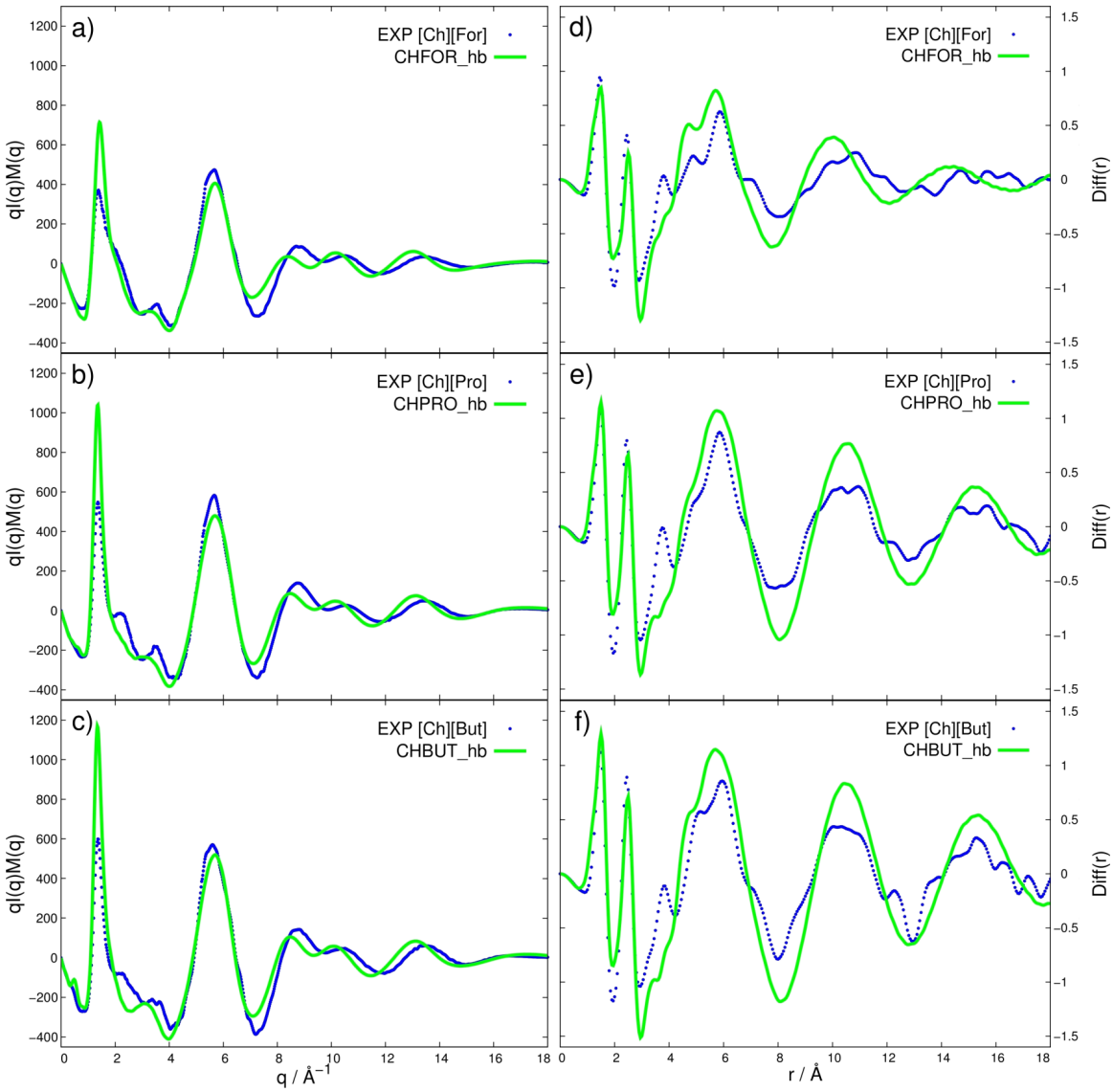

FIG. 7. Theoretical GAFF_HB and experimental $qI(q)M(q)$ and $Diff(r)$ of [Ch] [For], [Ch][Pro], and [Ch][But].

fit entirely the experimental intensities; (iii) the absence of prepeaks in the experimental curves is confirmed by theoretical features. Looking at the *Diff*(r) curves (Figures 7(d)–7(f)), we observe that the distances of most peaks are now quite well reproduced. However, with the exception of the intramolecular peaks, intensities of all peaks are not in full agreement with experiment. This seems to be consequence of the scarce agreement of the intensity of the main peak at 1.8 Å^{-1} in the structure factor. Looking again to the radial functions, we note that the experimental curves show a peak at about 3.8 Å inaccurately reproduced by our models. We could therefore conclude that introduction of this three-body term improves undoubtedly some aspect of the curves; on the other hand, some structural features continue to be quite far from experiment.

With the aim to clarify the origin of such discrepancies, we inspected several partial structure factors obtained from theoretical models. We observed that while the band at 4.5 Å is sum of various intramolecular and intermolecular contributions, the peak at 3.8 Å appears to be quite narrow, suggesting that highly correlated contributions are largely dominant. In addition, the cation seems to play a major role since the peak was observed in all the three compounds, although it is better defined in [Ch][But]. The only structural intramolecular parameter able to change during the simulations and really decisive on the *Diff*(r) curve is the NCCO dihedral angle of choline since it involves two atoms with high scattering factors. Any variation of NCCO angle changes the molecular conformation and affects the distance between the N and O atoms. Such intramolecular N $\cdots$ O distance can assume values close to 3.8 Å during conformational change and previous AIMD simulations revealed that conformational changes are indeed possible in the liquid.[24]

Choline conformation can be therefore studied by monitoring radial distribution functions between nitrogen (Ncho) and oxygen (Ocho) atoms of choline as shown in Figure 8. The two narrow peaks are associated to the N $\cdots$ O intramolecular distances of anti (3.78 Å) and gauche (3.2 Å) conformations. We can notice that for GAFF distributions, Figures 8(b), 8(e), and 8(h), the anticonformation is the preferred one, especially for [Ch][For], whereas when the three-body term is added to GAFF (GAFF_HB), Figures 8(c), 8(f), and 8(i), choline has no preferred conformations. As concerns AIMD results, Figures 8(a), 8(d), and 8(g), we observe that the Ncho-Ocho distribution of 9CHBUT presents a single and strong peak at 3.78 Å, corresponding to anticonformations, whereas 12CHFOR and 10CHPRO distributions show two peaks, the most intense of which associated again to anticonformations. *Ab initio* description gives therefore a conformational rigidity higher than that expected from classical models. As a matter of fact, gauche conformation was found as the lowest-energy structure for all the *ab initio* three ion-pairs and antiorientation was evaluated about 17 kJ/mol higher in energy. However, assuming different values for dielectric constant, gauche-anti relative stability was found to decrease[24] suggesting that flexibility of choline can be remarkably affected by the surrounding ions.

Radial distribution functions between choline nitrogen and carboxylate oxygen atoms (Ofor, Opro, Obut) can be useful to analyse secondary interactions in the different models. In

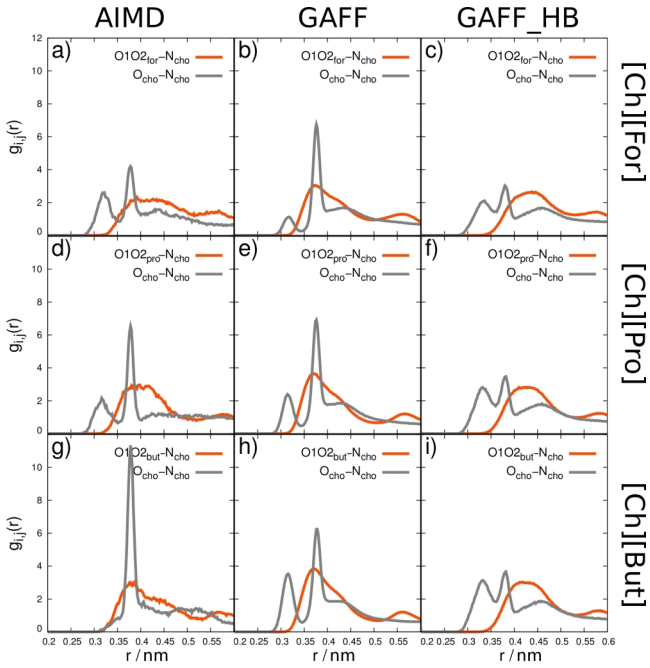

FIG. 8. Radial distribution functions of intramolecular oxygen-nitrogen distances of choline and intermolecular oxygen-nitrogen distances for the compounds.

GAFF simulations, these distribution functions show a broad band whose maximum overlaps with the peak corresponding to the anticonformation in the Ncho-Ocho distribution. On the contrary, GAFF_HB distributions show narrow bands centered at longer distances. AIMD gives results very similar to the GAFF distribution functions with a broad band whose maximum overlaps with the peak corresponding to anticonformation in the Ncho-Ocho distribution.

From our structural analysis, we can therefore conclude that the presence of the peaks at 3.8-4.5 Å in the experimental *Diff*(r) and their shape depend on three main structural features: hydrogen bond geometry, choline conformation, and secondary cation-anion contacts. In particular, intra- and inter-molecular N $\cdots$ O distances, whose contributions overlap in the *Diff*(r) curve, can complicate its assignment. Consequently, a good description of each contribution and the relative weight in the radial distribution functions affect drastically the whole shape of the curve. The satisfactory agreement obtained from AIMD description suggests that BioILs where ions are connected through Coulombic and hydrogen bonding interactions and where conformational aspects may condition the structural features need quantum mechanical methods for a complete description. We are confident that AIMD will give improvements to the study of liquid structures when it will be able to be applied to bigger systems.

V. CONCLUSIONS

In this work, we have reported energy dispersive X-ray diffraction data for a series of choline-based bio-ionic liquids. Different quantum-mechanical approaches have been followed to describe the liquid structure involving systems with different sizes: from the ion pairs to small portions of liquid. Theoretical results indicate that ions are connected by strong

hydrogen bonds. The typical oxygen-oxygen interaction mediated by the hydrogen bonding binds the ions in stable ion pairs in the liquid phase providing structures that are reminiscent of the isolated ionic couple found from *ab initio* geometrical optimizations. The acceptor-donor distance is about 2.6 Å with a sharp localization of the proton of choline around the oxygen atoms of the carboxylate group. The presence of well structured peaks in some intermolecular RDF, like N ⋯ O, reveals that the present ILs, as already found for choline aminoacid systems,[25] are substantially structured and cations and anions form alternating patterns in liquid.

The X-ray diffraction pattern has been successfully reproduced by *ab initio* MD simulations within the obvious spatial and temporal limits of the employed model. To extend such limits, the ionic liquids were studied by MD simulations based on classical potentials. Most of the structural features found from AIMD simulations are again present in classical description of liquid; for example, ions tend to form stable ion pairs through strong hydrogen bonding. However, one of the salient results is that the two-body force field, GAFF, as already observed for other protic ILs,[68] tends to overestimate cation-anion interactions with respect to the *ab initio* description; as a consequence, radial distribution functions obtained from this potential do not reproduce the experimental curve accurately, especially in the intermolecular distance range. Introduction of a three-body term in the force field actually weakens electrostatic interactions between ions although discrepancies with experiment continue to be observed, especially in reproducing intensities. We are aware that higher accuracy could be probably reached fitting a new set of force field parameters. Following this procedure, however, we risk to loose generality and transferability of force fields. *Ab initio* approach, although much more computationally demanding than classic methods, has the advantage to describe more accurately the different intermolecular interaction terms, such that, for example, the complex polarization effects typical of such systems. A subtle balance between intramolecular contributions, conformationally dependent, and intermolecular terms affects critically the whole radial distribution function. It is encouraging to observe that our *ab initio* approach successfully describes the X-Ray structure factors.

ACKNOWLEDGMENTS

We acknowledge the CINECA award under the ISCRA initiative, for the availability of high performance computing resources and support, grant DYNGEOM. The authors also thank Professor Ruggero Caminiti (Department of Chemistry, Rome Sapienza University) for providing free computing time on NARTEN Cluster HPC Facility.

[1]J. S. Wilkes, Green Chem. **4**, 73 (2002).
[2]E. W. Castner, Jr. and J. F. Wishart, J. Chem. Phys. **132**, 120901 (2010).
[3]P. Wasserscheid and W. Keim, Angew. Chem., Int. Ed. **39**, 3772 (2000).
[4]N. Gathergood, P. Scammells, and M. Garca, Green Chem. **8**, 156 (2006).
[5]M. Petkovic, K. R. Seddon, L. P. N. Rebelo, and C. S. Pereira, Chem. Soc. Rev. **40**, 1383 (2011).
[6]R. H. Broh-Kahn, Int. Rev. Med. **173**, 217 (1960).
[7]A. P. Abbott, G. Capper, D. L. Davies, H. L. Munro, R. K. Rasheed, and V. Tambyrajah, Chem. Commun. **2001**, 2010.
[8]A. P. Abbott, D. Boothby, G. Capper, D. L. Davies, and R. K. Rasheed, J. Am. Chem. Soc. **126**, 9142 (2004).
[9]J. Pernak, A. Syguda, I. Mirska, A. Pernak, J. Nawrot, A. Pradzynska, S. Griffin, and R. D. Rogers, Chem. Eur. J. **13**, 6817 (2007).
[10]J. Wilkes and M. Zaworotko, J. Chem. Soc., Chem. Commun. **1992**, 965.
[11]R. Lau, M. Sorgedrager, G. Carrea, F. Pantwijk, F. Secundo, and R. Sheldon, Green Chem. **6**, 483 (2004).
[12]K. Fukumoto, M. Yoshizawa, and H. Ohno, J. Am. Chem. Soc. **127**, 2398 (2005).
[13]K. Fukumoto and H. Ohno, Chem. Commun. **2006**, 3081.
[14]J. Kagimoto, K. Fukumoto, and H. Ohno, Chem. Commun. **2006**, 2254.
[15]G. Ou, M. Zhu, J. She, and Y. Yuan, Chem. Commun. **2006**, 4626.
[16]Y. Fukaya, Y. Iizuka, K. Sekikawa, and H. Ohno, Green Chem. **9**, 1155 (2007).
[17]N. Muhammad, M. I. Hossain, Z. Man, M. El-Harbawi, M. A. Bustam, Y. A. Noaman, N. B. M. Alitheen, M. K. Ng, G. Hefter, and C. Y. Yin, J. Chem. Eng. Data **57**, 2191 (2012).
[18]J. Restolho, J. L. Mata, and B. Saramago, Fluid Phase Equilib. **322-323**, 142 (2012).
[19]R. Klein, H. Dutton, O. Diat, G. J. T. Tiddy, and W. Kunz, J. Phys. Chem. B **115**, 3838 (2011).
[20]C. Russ and B. König, Green Chem. **14**, 2969 (2012).
[21]S. Aparicio and M. Atilhan, J. Phys. Chem. B **116**, 9171 (2012).
[22]S. Aparicio and M. Atilhan, J. Phys. Chem. C **116**, 12055 (2012).
[23]A. Benedetto, E. Bodo, L. Gontrani, P. Ballone, and R. Caminiti, J. Phys. Chem. B **118**, 2471 (2014).
[24]L. Tanzi, P. Benassi, M. Nardone, and F. Ramondo, J. Phys. Chem. A **118**, 12229 (2014).
[25]M. Campetella, E. Bodo, R. Caminiti, A. Martino, F. D'Apuzzo, S. Lupi, and L. Gontrani, J. Chem. Phys. **142**, 234502 (2015).
[26]M. Campetella, S. D. Santis, R. Caminiti, P. Ballirano, C. Sadun, L. Tanzi, and L. Gontrani, RSC Adv. **5**, 50938 (2015).
[27]A. Triolo, O. Russina, H. Bleif, and E. D. Cola, J. Phys. Chem. B **111**, 4641 (2007).
[28]C. S. Santos, H. V. R. Annapureddy, N. S. Murthy, H. K. Kashyap, E. W. Castner, Jr., and C. J. Margulis, J. Chem. Phys. **134**, 064501 (2011).
[29]H. K. Kashyap, C. S. Santos, N. S. Murthy, J. J. Hettige, K. Kerr, S. Ramati, J. Gwon, M. Gohdo, S. I. Lall-Ramnarine, J. F. Wishart, C. J. Margulis, and E. W. Castner, Jr., J. Phys. Chem. B **117**, 15328 (2013).
[30]H. K. Kashyap, J. J. Hettige, H. V. R. Annapureddy, and C. J. Margulis, Chem. Commun. **48**, 5103 (2012).
[31]H. V. R. Annapureddy, H. K. Kashyap, P. M. D. Biase, and C. J. Margulis, J. Phys. Chem. B **114**, 16838 (2010).
[32]K. Shimizu, C. E. S. Bernardes, and J. N. C. Lopes, J. Phys. Chem. B **118**, 567 (2014).
[33]O. Russina, L. Gontrani, B. Fazio, D. Lombardo, A. Triolo, and R. Caminiti, Chem. Phys. Lett. **493**, 259 (2010).
[34]O. Russina, A. Triolo, L. Gontrani, and R. Caminiti, J. Phys. Chem. Lett. **3**, 27 (2012).
[35]M. Macchiagodena, L. Gontrani, F. Ramondo, A. Triolo, and R. Caminiti, J. Chem. Phys. **134**, 114521 (2011).
[36]M. Macchiagodena, F. Ramondo, A. Triolo, L. Gontrani, and R. Caminiti, J. Phys. Chem. B **116**, 13448 (2012).
[37]V. Migliorati, P. Ballirano, L. Gontrani, A. Triolo, and R. Caminiti, J. Phys. Chem. B **115**, 4887 (2011).
[38]L. Gontrani, F. Ramondo, and R. Caminiti, Chem. Phys. Lett. **417**, 200 (2006).
[39]L. Gontrani, F. Ramondo, G. Caracciolo, and R. Caminiti, J. Mol. Liq. **139**, 23 (2007).
[40]L. Gontrani, R. Caminiti, L. Bencivenni, and C. Sadun, Chem. Phys. Lett. **301**, 131 (1999).
[41]R. Caminiti, M. Carbone, and C. Sadun, J. Mol. Liq. **75**, 149 (1998).
[42]M. Carbone, R. Caminiti, and C. Sadun, J. Mater. Chem. **6**, 1709 (1996).
[43]L. Gontrani, O. Russina, F. C. Marincola, and R. Caminiti, J. Chem. Phys. **131**, 244503 (2009).
[44]M. J. Frisch, G. W. Trucks, H. B. Schlegel, G. E. Scuseria, M. A. Robb, J. R. Cheeseman, G. Scalmani, V. Barone, B. Mennucci, G. A. Petersson *et al.*, GAUSSIAN 09, Revision C.01, Gaussian, Inc., Wallingford, CT, 2010.
[45]A. D. Becke, J. Chem. Phys. **98**, 5648 (1993).
[46]C. Lee, W. Yang, and R. Parr, Phys. Rev. B **37**, 785 (1988).
[47]W. Andreoni and A. Curioni, Parallel Comput. **26**, 819 (2000).
[48]J. P. Perdew, K. Burke, and M. Ernzerhof, Phys. Rev. Lett. **77**, 3865 (1996).
[49]I. C. Lin, M. D. Coutinho-Neto, C. Felsenheimer, O. A. von Lilienfeld, I. Tavernelli, and U. Rothlisberger, Phys. Rev. B **75**, 205131 (2007).

[50]N. Troullier and J. Martins, Phys. Rev. B **43**, 1993 (1991).
[51]S. Nosé, J. Chem. Phys. **81**, 511 (1984).
[52]S. Nosé, Mol. Phys. **52**, 255 (1984).
[53]W. G. Hoover, Phys. Rev. A **31**, 1695 (1985).
[54]J. Wang, R. M. Wolf, J. W. Caldwell, P. A. Kollman, and D. A. Case, J. Comput. Chem. **25**, 1157 (2004).
[55]E. Lindahl, B. Hess, and D. van der Spoel, J. Mol. Model. **7**, 306 (2001).
[56]L. Martinez, R. Andrade, E. G. Birgin, and J. M. Martinez, J. Comput. Chem. **30**, 2157 (2009).
[57]W. D. Cornell, P. Cieplak, C. I. Bayly, and P. A. Kollman, J. Am. Chem. Soc. **115**, 9620 (1993).
[58]P. Cieplak, W. D. Cornell, C. I. Bayly, and P. A. Kollman, J. Comput. Chem. **16**, 1357 (1995).
[59]W. D. Cornell, P. Cieplak, C. I. Bayly, I. R. Gould, K. M. Merz, Jr., D. M. Ferguson, D. C. Spellmeyer, T. Fox, J. W. Caldwell, and P. A. Kollman, J. Am. Chem. Soc. **117**, 5179 (1995).
[60]M. Parrinello and A. Rahman, Phys. Rev. Lett. **45**, 1196 (1980).
[61]M. Parrinello and A. Rahman, J. Appl. Phys. **52**, 7182 (1981).
[62]G. J. Martyna, D. J. Tobias, and M. L. Klein, J. Chem. Phys. **101**, 4177 (1994).
[63]S. L. Mayo, B. D. Olafson, and W. A. Goddard III, J. Phys. Chem. **94**, 8897 (1990).
[64]See supplementary material at http://dx.doi.org/10.1063/1.4931031 for Fig. S(a) presenting simulations at 300 K and 500 K for CHPRO and Fig. S(b) showing some simulations carried out scaling all atomic charges by 0.5 and other simulations performed starting from unchanged partial charge of isolated units and assuming zero only for atoms involved in hydrogen bond.
[65]I. T. Todorov, W. Smith, K. Trachenko, and M. T. Dove, J. Mater. Chem. **16**, 1911 (2006).
[66]T. G. A. Youngs, J. Comput. Chem. **31**, 639 (2010).
[67]C. J. Pings and J. Waser, J. Chem. Phys. **48**, 3016 (1968).
[68]L. Gontrani, E. Bodo, A. Triolo, F. Leonelli, P. D'Angelo, V. Migliorati, and R. Caminiti, J. Phys. Chem. B **116**, 13024 (2012).
[69]P. H. Gaskell and D. J. Wallis, Phys. Rev. Lett. **76**, 66 (1996).
[70]J. J. Hettige, H. K. Kashyap, H. V. R. Annapureddy, and C. J. Margulis, J. Phys. Chem. Lett. **4**, 105 (2013).
[71]J. J. Hettige, J. C. Araque, and C. J. Margulis, J. Phys. Chem. B **118**, 12706 (2014).
[72]M. Brehm and B. Kirchner, J. Chem. Inf. Model. **51**, 2007 (2001).
[73]B. H. Besler, K. M. Merz, and P. A. Kollman, J. Comput. Chem. **11**, 431 (1990).